

Compensating Position Drift in Time Domain Passivity Approach based Teleoperation

Vinay Chawda*
Department of Mechanical
Engineering
Rice University
Houston, TX 77005 USA

Ha Van Quang†
School of Mechanical
Engineering
Korea University of
Technology and Education
Cheonan, R. of Korea

Marcia K. O'Malley‡
Department of Mechanical
Engineering
Rice University
Houston, TX 77005 USA

Jee-Hwan Ryu§
School of Mechanical
Engineering
Korea University of
Technology and Education
Cheonan, R. of Korea

ABSTRACT

Passivity based approaches to bilateral teleoperation control ensure robust stability against disruptive effects of communication delays. These approaches, while achieving velocity tracking, cannot guarantee position tracking in general. Recently, the Time Domain Passivity Approach (TDPA) has been gaining interest in field of bilateral teleoperation due to its simplicity, ease of implementation, robustness to communication delays, and adaptive control design which promises less conservative performance than frequency domain passivity approaches. Several techniques have been proposed to counter the position drift with conventional passivity based approaches, but not much work has been done to address the problem of position drift with TDPA based control of teleoperation. We propose a novel position drift compensation architecture employing a virtual dependent energy source which leverages the passivity margins allowed by the communication channel to inject energy and recover position tracking without compromising system passivity. A drift compensation scheme is developed within this architecture that ensures synchronization of master and slave robot trajectories. The proposed method is generalizable to all bilateral teleoperation control architectures, and is robust against different communication delay and remote environment conditions. Experiments are conducted to validate the efficacy of the approach, and demonstrate position tracking with up to 1000 ms round-trip delays in free space motion and hard wall contact scenarios.

1 INTRODUCTION

Teleoperation over delayed communication channels has gained significant attention in the past two decades, with potential applications such as tele-surgery, tele-maintenance, search and rescue, and education [1]. Passivity is an attractive concept in dealing with time-delayed teleoperation due to its physically intuitive appeal. Passivity is a sufficient condition for stability, and has been a cornerstone of delayed teleoperation control. Furthermore, interconnected passive systems are passive [2], which is very convenient in analyzing passivity of interconnected systems such as master and slave manipulators and the communication channel typically present in a bilateral teleoperation system. In this paper we will restrict ourselves to passivity based approaches. Master and slave devices (without any local force-feedback) are always passive, but it has been shown in [3] that a communication channel with time-delay is not passive and may cause instability. Passivity based approaches, such as scattering approach [3] and wave variable approach [4], have been proposed to deal with the problem

of instability caused by time-delays in teleoperation. Many later schemes building on these two approaches have been proposed, and the reader is referred to [5] and [6] for a detailed survey of various passivity based schemes. Broadly, passivity based approaches can be divided in to frequency-domain and time-domain approaches. Frequency domain approaches, such as the scattering and wave variable approaches, have controller parameters which are fixed and are designed for the worst case scenario to dissipate any active energy generated by the communication channel. This leads to a conservative control design, and recently efforts have been made to formulate time-varying controller parameter schemes to improve performance [7], [8]. In [9], an energy based Time Domain Passivity Approach (TDPA) was proposed to monitor the system passivity via a *Passivity Observer* (PO) in real-time and adaptively tune the amount of energy dissipation through a *Passivity Controller* (PC) to enforce system passivity. TDPA carries the advantage of being adaptive by its very design over conventional passivity based approaches.

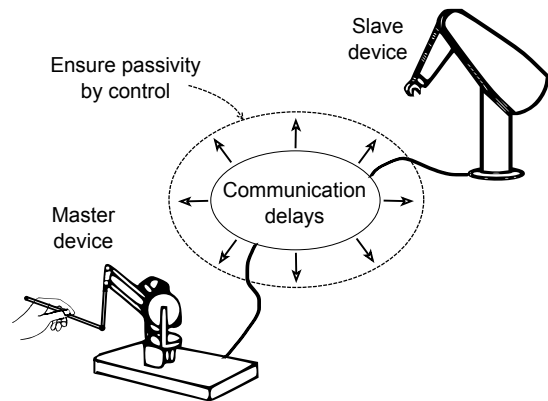


Figure 1: Communication delays are the main source of activity in bilateral teleoperation. Passivity based approaches aim to use control for passivating the communication channel, and hence ensure system passivity.

Most passivity based approaches only exchange force and velocity information between master and slave. The position controller on the slave side obtains the position command signal by integrating the velocity signal from the master. As a result, whenever there is a modification of the velocity command signal from the master to enforce passivity, or a mismatch in initial conditions, position drift develops between master and slave devices. Several approaches have been suggested to solve the problem of position drift in passivity based control of bilateral teleoperation with communication delays. In [10], wave integrals are transmitted over communication channel which carry position information. In [11] and [12], explicit position information is sent over communication channel and position coupling controllers enforce position tracking. A new

*e-mail: vinay.chawda@rice.edu

†e-mail: quang.hut@gmail.com

‡e-mail: omalleym@rice.edu

§e-mail: jhryu@kut.ac.kr

signal encoding position information with velocity was proposed in [13] and [14] to be sent over the communication channel instead of plain velocity signal. In [15], an energy injection based scheme was proposed to compensate position drift in TDPA based bilateral teleoperation control, where additional energy is injected whenever passivity gaps are presented by the communication channel to emulate *lossless* communication.

In this paper, we propose an approach utilizing the newly proposed Time Delay Power Network (TDPN) representation [16] to counter position drift in TDPA based control of bilateral teleoperation systems. Although time delay in the communication channel is a source of activity, it does not produce energy all the time. We extend the classic TDPA based control by introducing a virtual energy source that injects energy whenever the communication channel is passive. By leveraging such passivity gaps, our method ensures that position drift is brought to null. Our proposed method differs from earlier approaches to compensate position drift on several important points:

- Proposed method is based on TDPN formulation, making it generalizable to position-measured force bilateral teleoperation architecture
- Position synchronization can be achieved under time-varying communication delays
- Freedom of implementing energy injection schemes without affecting system passivity allows possibility of developing different drift compensation schemes within the proposed architecture

This paper presents a general method for compensating position drift under TDPA based bilateral teleoperation control, that is robust of communication delays (small, large, and variable), types of remote environment interactions (free space, hard wall contact) and is applicable to all bilateral teleoperation architectures. The efficacy of the method is validated experimentally on a dual-PHANToM teleoperation setup.

2 TDPA USING NETWORK REPRESENTATION

In this section we briefly review the framework presented in [16] and [17] for TDPA based bilateral control of delayed teleoperation systems. Figure 2 shows the block diagram representation of the bilateral teleoperation system considered in this paper.

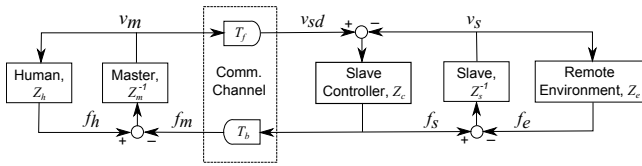


Figure 2: Block diagram representation of a position-computed force bilateral teleoperation system with communication delays.

The bilateral teleoperation system shown in Fig. 2 can be represented as a network composed of subsystems exchanging force and velocity signals, as shown in Fig. 3. Using TDPN formulation described in [16], we can further describe the bilateral teleoperation system in electrical network representation as shown in Fig. 4. The basic idea behind TDPN formulation is to identify the cause for command and feedback flow and effort signals, and represent them by corresponding ideal flow and effort sources. TDPN is a 2-port network characterizing the delay needed by signals to travel from one port to another.

2.1 Passivity analysis and control using TDPA

It is a well-established result that passivity of a teleoperator two-port network is sufficient to guarantee stable bilateral teleoperation

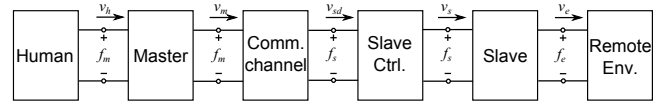


Figure 3: Network representation of a position-computed force bilateral teleoperation system with communication delays.

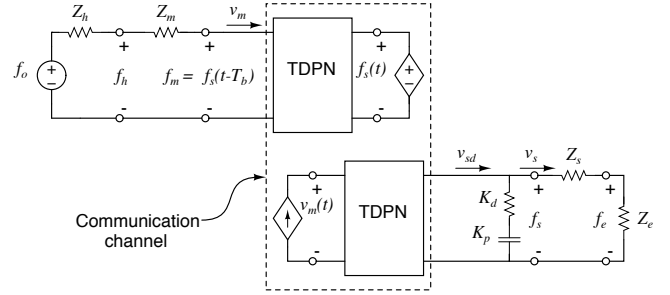


Figure 4: Electrical network representation of the bilateral teleoperation system using TDPN formulation.

interaction [18]. Passivity of the bilateral teleoperation system is ensured if the individual subsystems forming the system as shown in Fig. 3 are passive. The only subsystem whose passivity is not guaranteed is the communication channel. As shown in Fig. 4, the communication channel is composed of two TDPNs, which if made passive individually, will make the communication passive and hence ensure system passivity. In the following we will describe how TDPA can be used to make the TDPNs passive, thus ensuring stable bilateral teleoperation.

TDPA has two main components: a *Passivity Observer* (PO) which monitors the energy flow of the network, and a *Passivity Controller* (PC) which dissipates the energy introduced by the active elements in the network. It is assumed that the sampling rate is substantially faster than the dynamics of the system, and the changes in force and velocity within each sampling period are small.

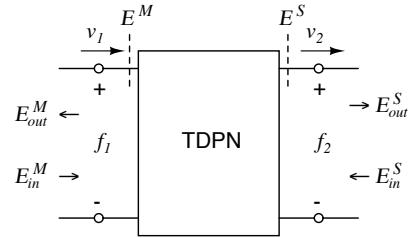


Figure 5: Energy flow in a TDPN. The right and left port energy flows are further separated into input and output energy flows.

The energy flow of the TDPN is given by:

$$E_N(k) = E^M(k) + E^S(k), \quad \forall k \geq 0 \quad (1)$$

where $E^M(k)$ and $E^S(k)$ are the right and left port energy contributions given as:

$$E^M(k) = \Delta T \sum_{j=0}^k f_1(j)v_1(j) \quad \text{and} \\ E^S(k) = \Delta T \sum_{j=0}^k f_2(j)v_2(j), \quad \forall k \geq 0 \quad (2)$$

where ΔT is the sampling period.

The right and left port energy contributions are further split into input and output energy flows that come in and out of the network, as shown in Fig. 5 ([17], [16]), and given as:

$$\begin{aligned} E^M(k) &= E_{in}^M(k) - E_{out}^M(k), \quad \forall k \geq 0 \\ E^S(k) &= E_{in}^S(k) - E_{out}^S(k), \quad \forall k \geq 0 \end{aligned} \quad (3)$$

The passivity condition for the TDPN is given by

$$E^N(k) = E^M(k) + E^S(k) \geq 0, \quad \forall k \geq 0 \quad (4)$$

but since $E^M(k)$ and $E^S(k)$ are not observable at the same time due to time-delay, this passivity condition cannot be checked in real-time in an experimental setup. To overcome this limitation, an algebraic work around was proposed in [17] to decouple the passivity condition (4) into a set of observable passivity conditions.

Combining equations (3) and (4), we can rewrite the passivity condition as:

$$\begin{aligned} E^N(k) &= E_{in}^M(k) - E_{out}^M(k) + E_{in}^S(k) - E_{out}^S(k) \\ &= E^{L2R}(k) + E^{R2L}(k) \geq 0, \quad \forall k \geq 0 \end{aligned} \quad (5)$$

where,

$$\begin{aligned} E^{L2R}(k) &= E_{in}^M(k) - E_{out}^S(k), \text{ and} \\ E^{R2L}(k) &= E_{in}^S(k) - E_{out}^M(k) \end{aligned} \quad (6)$$

are the *decoupled* energy flows from left-to-right and right-to-left ports of the network. The passivity condition (5) will be satisfied if $E^{L2R}(k) \geq 0$ and $E^{R2L}(k) \geq 0$ are satisfied. Taking time delay into account, the *observable* passivity conditions can be written as:

$$\begin{aligned} E_{obs}^{L2R}(k) &= E_{in}^M(k - T_f(k)) - E_{out}^S(k) \geq 0, \quad \forall k \geq 0, \\ E_{obs}^{R2L}(k) &= E_{in}^S(k - T_b(k)) - E_{out}^M(k) \geq 0, \quad \forall k \geq 0. \end{aligned} \quad (7)$$

Please refer to [16] for a detailed proof of (7). Physically, the passivity condition (7) means that the energy output at a port is always upper bounded by the input energy at the opposite port, and vice versa.

2.1.1 Passivity Observer

Passivity observer is real-time computation of the passivity condition (7), taking into account any energy dissipated by the passivity controller. The two passivity observers for each port of the network are given as:

$$\begin{aligned} W_M(k) &= E_{in}^S(k - T_b(k)) - E_{out}^M(k) + E_{PC}^M(k - 1), \text{ and} \\ W_S(k) &= E_{in}^M(k - T_f(k)) - E_{out}^S(k) + E_{PC}^S(k - 1). \end{aligned} \quad (8)$$

E_{PC}^M and E_{PC}^S are the energy corrections introduced by the passivity controllers, and are defined later in (11) and (14).

2.1.2 Passivity Controller

The Passivity Controller (PC) is a variable damper which bounds the output energy of a port by the input energy from the opposite port by dissipating any extra energy.

In impedance configuration (Fig. 6(a)), the PC takes the following form:

$$f_m(k) = \hat{f}_m(k) + \alpha(k)v_m(k) \quad (9)$$

where $\hat{f}_m(k) = f_s(k - T_b(k))$ is the *untouched* force signal coming from the slave. The coefficient $\alpha(k)$ is given as:

$$\alpha(k) = \begin{cases} 0 & \text{if } W^M(k) > 0 \\ -\frac{W^M(k)}{\Delta T v_m^2(k)} & \text{else, if } |v_m(k)| > 0 \end{cases} \quad (10)$$

and the energy dissipated by the PC is given as:

$$E_{PC}^M(k) = \Delta T \sum_{j=0}^k \alpha(j)v_m^2(j) \quad (11)$$

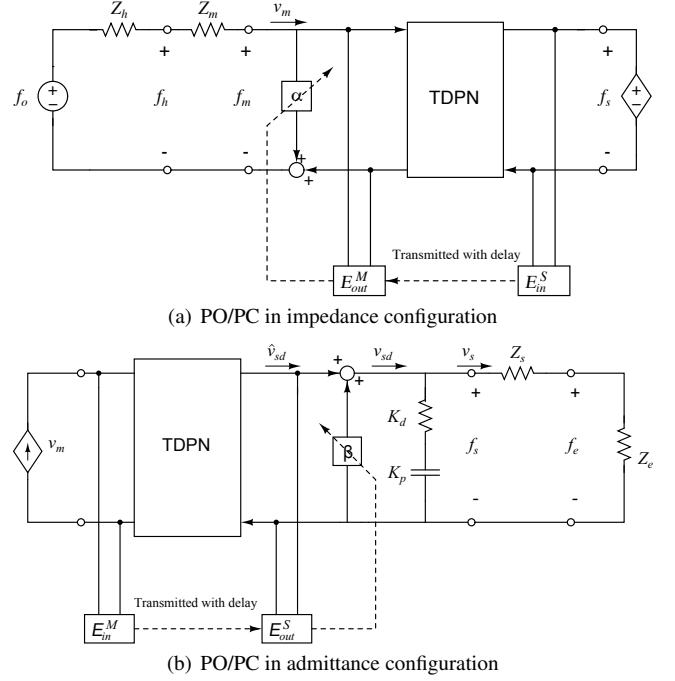


Figure 6: Passivated TDPN with PO/PC. Note that PC is not required on the ports connected to the ideal sources.

In admittance configuration (Fig. 6(b)), the PC takes the form:

$$v_{sd}(k) = \hat{v}_{sd}(k) + \beta(k)f_s(k) \quad (12)$$

where $\hat{v}_{sd}(k) = v_m(k - T_f(k))$ is the *untouched* velocity signal coming from the master. The coefficient $\beta(k)$ is given as:

$$\beta(k) = \begin{cases} 0 & \text{if } W^S(k) > 0 \\ -\frac{W^S(k)}{\Delta T f_s^2(k)} & \text{else, if } |f_s(k)| > 0 \end{cases} \quad (13)$$

and the energy dissipated by the PC is given as:

$$E_{PC}^S(k) = \Delta T \sum_{j=0}^k \beta(j)f_s^2(j) \quad (14)$$

See [9] and [19] for a more detailed proof and derivation of TDPA.

2.1.3 Passivity of ideal flow and effort sources

The analysis in Sec. 2.1.2 described placing PO/PC on both ports of a general TDPN to enforce passivity. In the special case when one port of a TDPN is attached to an ideal flow or effort source, passivity needs to be enforced only on the opposite port, since an ideal source can absorb infinite amount of energy. Any change in flow signal will not affect the ideal effort source, and similarly any change in effort across an ideal flow source will have no effect. Hence any active energy generated at the TDPN and traveling towards the ideal source will not affect the system passivity, and only a PC at the opposite port is required to passivate the TDPN.

2.2 Cause of position drift

Ideally, the slave controller should act on the position error between delayed master position (*desired position*) and slave position. However, since position and force signals are not power correlated, velocity signal is transmitted over the communication channel. The position command to the slave controller $x_{sd}(k)$ is then obtained by integrating the transmitted velocity $v_{sd}(k)$ as:

$$x_{sd}(k) = \Delta T \sum_{j=0}^k v_{sd}(j). \quad (15)$$

The slave PC has admittance causality as shown in Fig. 6(b) and modifies untouched delayed master velocity $\hat{v}_{sd}(k)$ to dissipate energy as given by (12). Thus, the modified position command signal for the slave controller incurs drift given as:

$$\begin{aligned} x_{err}(k) &= \Delta T \sum_{j=0}^k (v_{sd}(j) - \hat{v}_{sd}(j)) \\ &= \Delta T \sum_{j=0}^k \beta(j) f_s(j). \end{aligned} \quad (16)$$

Thus, whenever slave PC is active ($\beta(k) \neq 0$ and $f_s(k) \neq 0$) position drift is accumulated. Due to integral action, position drift is the cumulative result of all previous slave side PC corrections. Thus, passivity on the slave side is ensured at the cost of introducing position drift between master and slave devices. Figure 7 shows the position drift typically observed in TDPA based control, where x_m is the master position and x_s is the slave position.

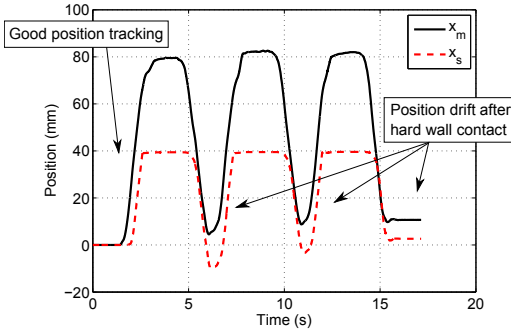


Figure 7: Position drift incurred during hard wall contact with TDPA based control. Round trip communication delay was 200ms.

3 ENERGY INJECTION TO COMPENSATE FOR POSITION DRIFT

Position drift is due to velocity modification by the slave PC, which happens whenever energy is generated at the slave side port due to active behavior of the communication channel. The slave side port of the communication channel is not always active though, and there are instants when the channel is passive and dissipates energy as shown in Fig. 8.

These instants of over-dissipation are used to inject energy in a way that counters the position drift due to previous PC corrections. The net result is that on the slave side port of the communication channel no energy generation is allowed by the slave PC and energy dissipation by the PC is countered by the additional energy injection. In electrical network representation, we inject energy by use of a dependant flow source, whose value is determined by the position drift. The scheme is shown in Fig. 9. The energy injected is always bound by the slave side PO/PC, hence ensuring system passivity.

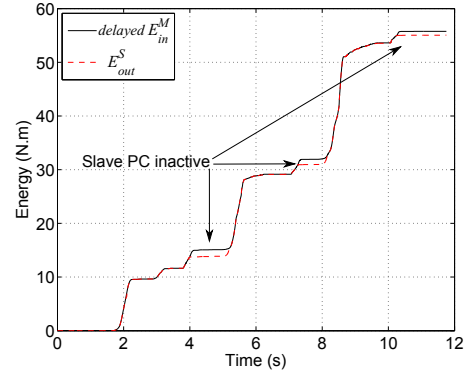


Figure 8: Slave PC ensures that output energy at the slave side is always bounded by the input energy at the master side. There are instants though when the net energy flow towards slave side is positive and slave PC is inactive (colored regions).

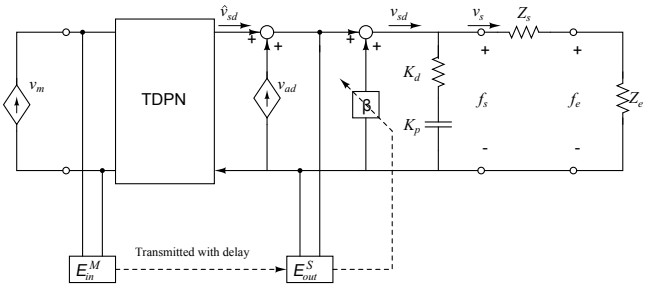


Figure 9: Energy injection via a dependant flow source to compensate for the position drift. Slave PO/PC passivates both the TDPN and the additional flow source.

We propose the following scheme for the dependant flow source $v_{ad}(k)$:

$$v_{ad}(k) = \frac{1}{\Delta T} \left(\hat{x}_{sd}(k) - \Delta T \sum_{j=0}^{k-1} v_{sd}(j) - \hat{v}_{sd}(k) \Delta T \right) \quad (17)$$

where, $\hat{x}_{sd}(k) = x_m(k - T_f(k))$ is the delayed master position signal, $v_{sd}(k)$ is the desired velocity command to the slave controller, $\hat{v}_{sd}(k) = v_m(k - T_f(k))$ is the delayed master velocity and ΔT is the sampling period. The flow source $v_{ad}(k)$ as described by (17) generates a flow which negates the net position drift incurred up to $(k-1)^{th}$ time instant.

3.1 Passivity Analysis

Passivity analysis is similar to regular TDPA based control, but with the slight modification that instead of just passivating the TDPN attached to the slave side, we passivate both the TDPN and additional flow source as shown in Fig. 10.

The master and slave side energy contributions given by (2) are now replaced by

$$\begin{aligned} E^M(k) &= \Delta T \sum_{j=0}^k f_{md}(j) v_m(j) \quad \text{and} \\ E^S(k) &= \Delta T \sum_{j=0}^k f_s(j) (\hat{v}_{sd}(j) + v_{ad}(j)). \end{aligned} \quad (18)$$

The remainder of the analysis is carried out as described in Section 2.1.

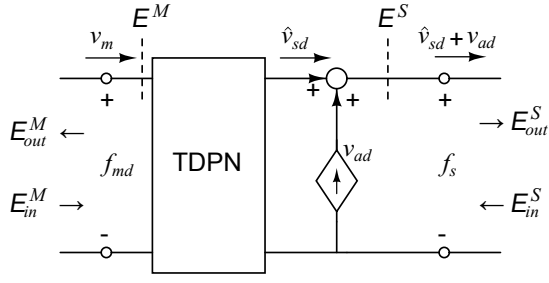


Figure 10: The TDPN attached to the slave side is passivated along with the additional flow source.

We described one scheme for designing the flow source $v_{ad}(k)$, but schemes other than (17) can also be used for the flow source and compensate for position drift, since the proposed approach ensures passivity regardless of $v_{ad}(k)$. Regular TDPN without drift compensation can be obtained as a special case when $v_{ad}(k) = 0, \forall k \geq 0$.

3.2 Compensation of position drift

As an example, we will illustrate how the energy injection scheme with the additional flow source given by (17) compensates position drift in the case of constant delays and no packet loss.

In case of constant time delay, we can write:

$$\hat{x}_{sd}(k) = \Delta T \sum_{j=0}^k \hat{v}_{sd}(j). \quad (19)$$

Using (19), we can rewrite (17) as:

$$\begin{aligned} v_{ad}(k) &= \sum_{j=0}^{k-1} (\hat{v}_{sd}(j) - v_{sd}(j)) \\ \Rightarrow v_{ad}(k) - v_{ad}(k-1) &= \hat{v}_{sd}(k-1) - v_{sd}(k-1) \\ \Rightarrow v_{ad}(k) &= \hat{v}_{sd}(k-1) + v_{ad}(k-1) - v_{sd}(k-1) \end{aligned} \quad (20)$$

Referring to Fig. 9, (12) can be rewritten as:

$$v_{sd}(k) = \hat{v}_{sd}(k) + v_{ad}(k) + \beta(k)f_s(k) \quad (21)$$

Thus, from (20) and (21) we get

$$v_{ad}(k) = -\beta(k-1)f_s(k-1). \quad (22)$$

Recomputing the position drift from Section 2.2 as:

$$\begin{aligned} x_{err}(k) &= \Delta T \sum_{j=0}^k (v_{sd}(j) - \hat{v}_{sd}(j)) \\ &= \Delta T \sum_{j=0}^k (\hat{v}_{sd}(j) + v_{ad}(j) + \beta(j)f_s(j)) - \Delta T \sum_{j=0}^k \hat{v}_{sd}(j) \\ &= \Delta T \sum_{j=0}^k v_{ad}(j) + \Delta T \sum_{j=0}^k \beta(j)f_s(j) \\ &= -\Delta T \sum_{j=0}^{k-1} \beta(j)f_s(j) + \Delta T \sum_{j=0}^k \beta(j)f_s(j) \\ &= \Delta T \beta(k)f_s(k) \end{aligned} \quad (23)$$

Comparing (23) with the expression for position drift given in (16), it can be observed that there is no more accumulation of position drift due to integral action. Whenever slave PC is inactive ($\beta(k) = 0$), position drift $x_{err}(k)$ is brought to null. The same result can be obtained for the time-varying delay case also, but the analysis is slightly more involved as equation (19) will have additional terms resulting from variable delay.

4 EXPERIMENTAL IMPLEMENTATION ON A DUAL-PHANTOM SETUP

Experiments were performed using two PHANToM Premium 1.5 devices controlled using the same computer at a sampling rate of 1 kHz, and communication delay was simulated in software. Figure 11 shows the dual PHANToM teleoperation setup. The devices were calibrated before the experiments to remove any initial position mismatch. A position-force bilateral control architecture was used, with delayed slave control force used as the feedback force to the master and a position PD controller at the slave side to make the slave follow master position commands.

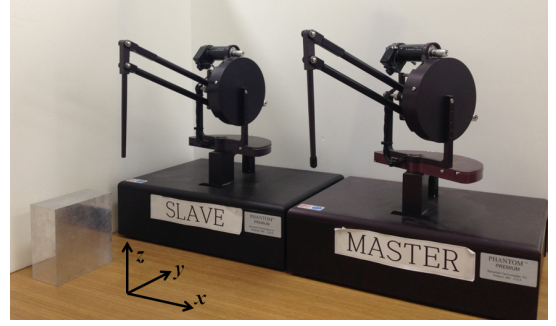


Figure 11: Dual PHANToM teleoperation setup used for the experiments. Dominant motion was along the x -axis.

A passive virtual mass-spring system was implemented on the master side to prevent high frequency force fluctuations due to master PC action [17]. This virtual mass-spring system acts as a bi-directional filter, filtering out the sudden force changes caused by the master PC and transmitting only the low frequency components to the operator. The velocity command from the operator is also filtered and only low frequency components are transmitted to slave side. The effect of filtering can be negligible if virtual mass values (m_c) are selected to be very small and virtual spring values (k_c) very high, thus increasing the cutoff frequency of this bi-directional filter. The parameters were tuned such that cutoff frequency was smaller than the high frequency fluctuations caused by the PC action. For the experiments, virtual mass was 0.0001 kg and virtual spring stiffness 1000 N/m. Figure 12 shows the complete teleoperation scheme with the proposed drift compensator on the slave side and a virtual mass-spring system at the master side.

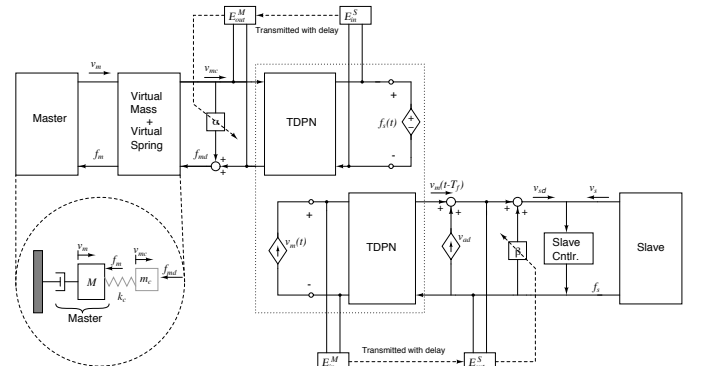


Figure 12: Time delayed teleoperator with the proposed position drift compensation scheme.

Experiments were conducted with regular TDPN and with the proposed drift compensation approach under free space motion and

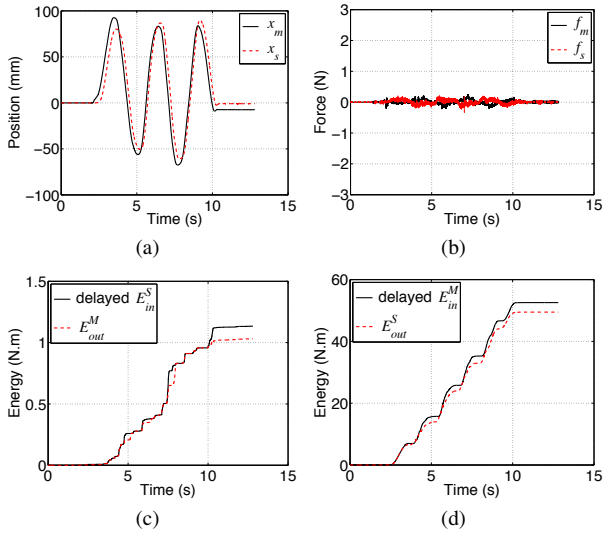


Figure 13: $T_{rt} = 200$ ms, free space motion without drift compensation

hard wall contact conditions to demonstrate the efficacy of the proposed approach. Experiments were repeated for a communication round-trip delay of $T_{rt} = T_f + T_b = 200$ ms, and also with a larger 1000 ms round-trip delay to demonstrate the robustness of the approach. Please note that teleoperation without TDPA was unstable for all the above cases, and those plots are omitted here due to limited space. See [17] for detailed comparative analysis of teleoperation with TDPA and without TDPA. Only x -direction signals are plotted, since dominant motion was along this axis only. Each figure is divided into four subplots showing: (a) Master and slave positions, (b) Master and slave control forces, (c) Output energy at the master and delayed input energy from the slave, and (d) Output energy at the slave and delayed input energy from the master. Additional energy injected (E_{ad}) by the flow source before PC is also included in figures showing plots for the drift compensation cases.

Figure 13 shows free space motion with 200 ms round trip delay and without drift compensation. Position drift can be observed in Fig. 13(a). The experiment was repeated with drift compensation and plots in Fig. 14(a) demonstrate that position synchronization between master and slave is achieved. In Fig. 14(b), a spike in master control force is observed before $t = 3$ s, which corresponds to the moment of drift compensation as seen by E_{ad} plot in Fig. 14(d).

Figures 15 and 16 show hard wall contact experiments without drift compensation and with drift compensation respectively, with a round trip delay of 200ms. Comparing Figs. 15(a) and 16(a), it can be observed that the proposed approach can effectively compensate for the position drift in hard wall contact scenario. Some sudden force spikes were felt in free space (Fig. 16(b)) when drift compensation occurred. Such force spikes occur when the slave PC has been active for some time and significant position drift has been accumulated, such as during contact with a hard wall.

In Figs. 17 and 18, results from free space motion experiments with 1000 ms round trip delay are shown. It can be seen in Fig. 17(d) that with such a large communication delay, the slave PC is active most of the time (slave PC keeps the output energy from slave upper bounded by the input energy from master), causing significant position drift as shown in Fig. 17(a). It can be seen that slave position has very little correspondence to master position commands, and large master device movements were required to elicit a response from slave. The experiment was repeated with drift compensation turned on, and it can be seen in Fig. 18(a) that there is no position drift between master and slave device positions.

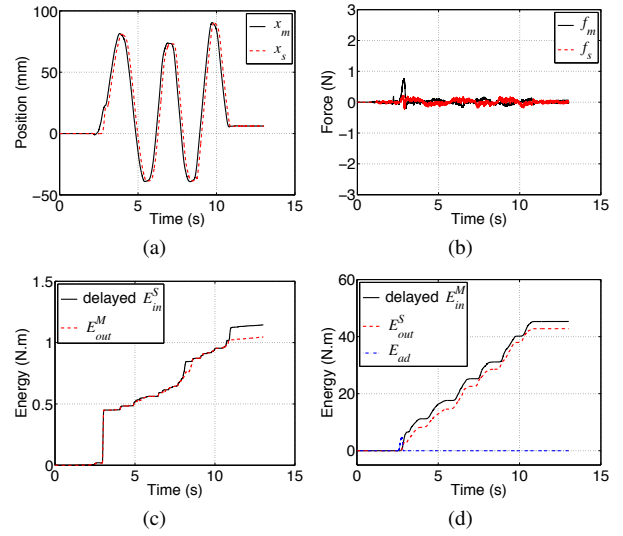


Figure 14: $T_{rt} = 200$ ms, free space motion with drift compensation

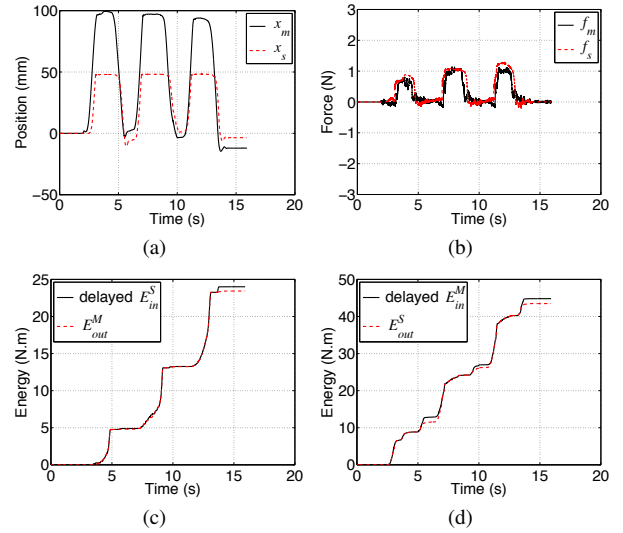


Figure 15: $T_{rt} = 200$ ms, hard wall contact without drift compensation

Few force spikes were observed (Fig. 18(b)) when drift compensation happened, which typically follows the time instants when the direction of motion is suddenly reversed.

Hard wall contact experiments were conducted with 1000 ms round trip delay, and Figs. 19 and 20 show the results without and with drift compensation respectively. In Fig. 19(a), it can be seen that large communication delay and hard wall contact have resulted in significant position drift. The master had to be moved significantly (> 120 mm penetration) to bring the slave in contact with the wall, and even then the feeling of wall was soft, as demonstrated by the master control force in Fig. 19(b). When the same experiment was repeated with drift compensation turned on, slave position followed master device position closely and resulted in no position drift at steady state as shown in Fig. 20(a). Small penetrations by the master inside the wall boundary (~ 50 mm) were sufficient for generating a noticeable feedback force (see Fig. 20(b)). Again, force spikes were observed when master was coming out of a hard wall interaction due to immediate position compensation affected by the drift compensator.

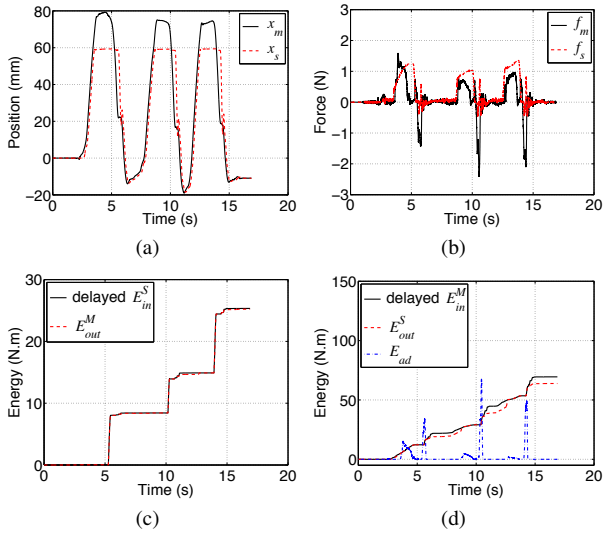


Figure 16: $T_{rt} = 200$ ms, hard wall contact with drift compensation

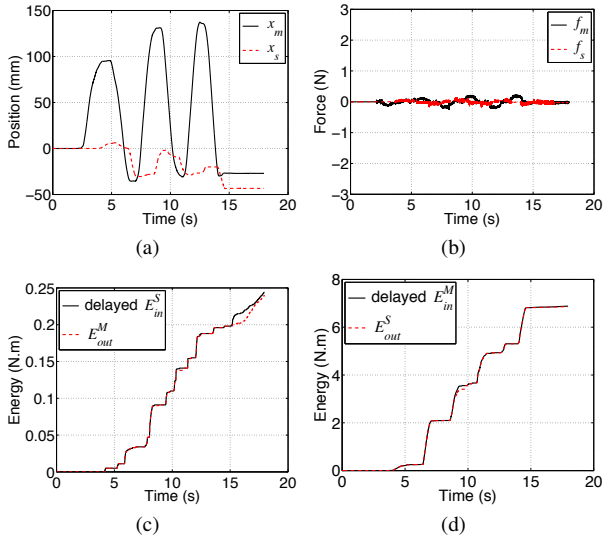


Figure 17: $T_{rt} = 1000$ ms, free space motion without drift compensation

5 CONCLUSIONS

Position drift between master and slave devices is a common artifact of passivity based bilateral teleoperation control with communication delays. Modifications in commanded velocity from master due to passivity controller are accumulated over time resulting in position drift. The proposed method is based on injecting additional energy to compensate for position drift between master and slave devices in teleoperation under TDPA. The energy is injected by a virtual dependent energy source whenever the communication channel presents passivity gaps. The additional energy injected is bounded by the slave PC, thus ensuring system passivity (and hence stability) at all times.

The results from experiments conducted on the dual-PHANToM setup under different remote environment interaction conditions (free space and hard wall contact), and under different communication channel conditions (200 ms and 1000 ms round-trip delays) establish the efficacy and robustness of the proposed approach in compensating position drift. Although the experiments shown here

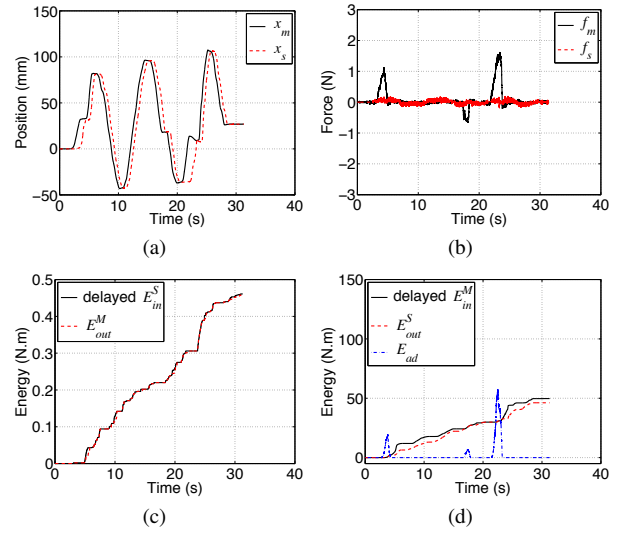


Figure 18: $T_{rt} = 1000$ ms, free space motion with drift compensation

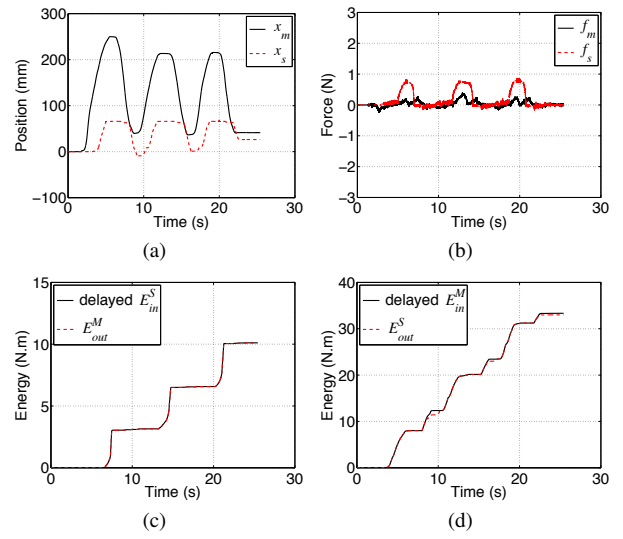


Figure 19: $T_{rt} = 1000$ ms, hard wall contact without drift compensation

are with constant communication delays, the method is equally applicable to variable communication delays and communication black-out scenarios.

A position drift compensation scheme for teleoperation under TDPA was proposed in [15], which described an approach based on injecting energy to compensate the position drift. The approach proposed in this paper also uses the idea of injecting energy, but with some key differences. First, our approach is based on TDPN formulation, which facilitates extension of the proposed method to position-measured force teleoperation architecture [16]. Second, in our approach we keep the classic PC formulation, and inject energy via a virtual dependent flow source. This has the dual benefits of keeping the simple classic PC formulation, and separating energy injection from PC, thereby giving freedom of implementing any compensation scheme within the proposed method. We suggested one scheme of designing the virtual dependent flow source, but other schemes are also possible which will achieve drift compensation. Nevertheless, the proposed method has some limitations which require further study. In situations such as hard wall contact

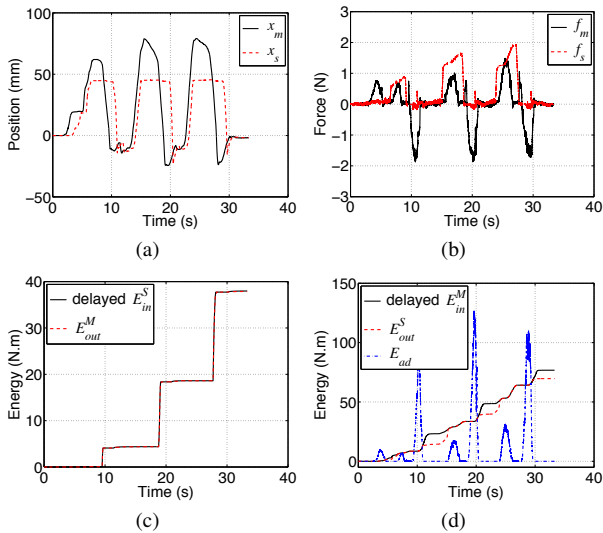


Figure 20: $T_{rt} = 1000$ ms, hard wall contact with drift compensation

or sudden reversal of direction of motion, slave PC is active for a long period before a passivity gap presents itself. This causes an immediate correction of a large accumulated position drift, resulting in a force spike felt at the master side. Such force spikes affect the free space motion feeling. Future work will involve designing a drift compensation scheme to minimize force spikes in free space motion and extend the method to improve force reflection at the master side.

ACKNOWLEDGEMENTS

The authors gratefully acknowledge the financial support from IEEE Technical Committee on Haptics 2013 Student Exchange Program for Cross-Disciplinary Fertilization. This work was supported in part by NSF Grant CNS-1136099 and the project (Development of a Tele-Service Engine and Tele-Robot Systems with Multi-Lateral Feedback) funded by the Ministry of Trade, Industry & Energy of Korea.

REFERENCES

- [1] G. Niemeyer, C. Preusche, and G. Hirzinger. *Springer Handbook of Robotics, Chapter 31 - Telerobotics*. Springer, 2008.
- [2] H. K. Khalil. *Nonlinear systems*, volume 3. Prentice hall Upper Saddle River, 2002.
- [3] R. Anderson and M.W. Spong. Bilateral control of teleoperators with time delay. *IEEE Transactions on Automatic Control*, 34(5):494–501, 1989.
- [4] G. Niemeyer and J.-J.E. Slotine. Stable adaptive teleoperation. *IEEE Journal of Oceanic Engineering*, 16(1):152–162, 1991.
- [5] P. F. Hokayem and M.W. Spong. Bilateral teleoperation: An historical survey. *Automatica*, 42(12):2035 – 2057, 2006.
- [6] P. Arcara and C. Melchiorri. Control schemes for teleoperation with time delay: A comparative study. *Robotics and Autonomous Systems*, 38(1):49–64, 2002.
- [7] N.A. Tanner and G. Niemeyer. Online tuning of wave impedance in telerobotics. In *IEEE Conference on Robotics, Automation and Mechatronics*, pages 7–12, 2004.
- [8] E.J. Rodriguez-Seda and M.W. Spong. A time-varying wave impedance approach for transparency compensation in bilateral teleoperation. In *IEEE/RSJ International Conference on Intelligent Robots and Systems (IROS)*, pages 4609–4615, 2009.
- [9] J. Ryu, D. Kwon, and B. Hannaford. Stable teleoperation with time-domain passivity control. *IEEE Transactions on Robotics and Automation*, 20(2):365–373, 2004.

- [10] G. Niemeyer and J.-J.E. Slotine. Towards force-reflecting teleoperation over the internet. In *IEEE International Conference on Robotics and Automation (ICRA)*, volume 3, pages 1909–1915 vol.3, 1998.
- [11] D. Lee and M. W. Spong. Passive bilateral teleoperation with constant time delay. *IEEE Transactions on Robotics*, 22(2):269–281, 2006.
- [12] N. Chopra, M.W. Spong, R. Ortega, and N.E. Barabanov. On tracking performance in bilateral teleoperation. *IEEE Transactions on Robotics*, 22(4):861–866, 2006.
- [13] N. Chopra, M. W. Spong, and R. Lozano. Synchronization of bilateral teleoperators with time delay. *Automatica*, 44(8):2142–2148, 2008.
- [14] D. Lee and D. Xu. Feedback r-passivity of lagrangian systems for mobile robot teleoperation. In *IEEE International Conference on Robotics and Automation (ICRA)*, pages 2118–2123, 2011.
- [15] J. Artigas, J. Ryu, and C. Preusche. Position drift compensation in time domain passivity based teleoperation. In *IEEE/RSJ International Conference on Intelligent Robots and Systems (IROS)*, pages 4250–4256, 2010.
- [16] J. Artigas, J. Ryu, C. Preusche, and G. Hirzinger. Network representation and passivity of delayed teleoperation systems. In *IEEE/RSJ International Conference on Intelligent Robots and Systems (IROS)*, pages 177–183, 2011.
- [17] J. Ryu, J. Artigas, and C. Preusche. A passive bilateral control scheme for a teleoperator with time-varying communication delay. *Mechatronics*, 20(7):812 – 823, 2010.
- [18] R. J. Anderson and M. W. Spong. Asymptotic stability for force reflecting teleoperators with time delay. *The International Journal of Robotics Research*, 11(2):135–149, 1992.
- [19] B. Hannaford and J. Ryu. Time-domain passivity control of haptic interfaces. *IEEE Transactions on Robotics and Automation*, 18(1):1–10, 2002.